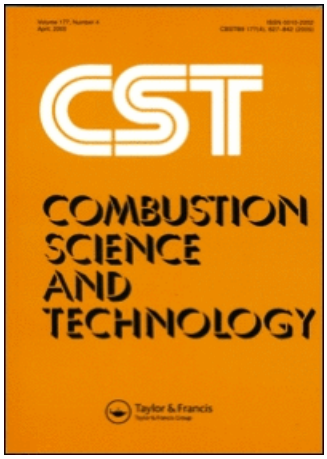

Combustion Science and Technology
Publication details, including instructions for authors and subscription information:
http://www.informaworld.com/smpp/title~content=t713456315

Time Dependent Operator-split and Unsplit Schemes for One Dimensional Premixed Flames

G. Goyal [a]; P. J. Paul [a]; H. S. Mukunda [a]; S. M. Deshpande [a]
[a] Department of Aerospace Engineering. Indian Institute of Science, Bangalore, India

Online Publication Date: 01 August 1988
To cite this Article: Goyal, G., Paul, P. J., Mukunda, H. S. and Deshpande, S. M. (1988) 'Time Dependent Operator-split and Unsplit Schemes for One Dimensional Premixed Flames', Combustion Science and Technology, 60:1, 167 - 189
To link to this article: DOI: 10.1080/00102208808923983
URL: http://dx.doi.org/10.1080/00102208808923983

Combust. Sci. and Tech., 1988, Vol. 60, pp. 167–189
Photocopying permitted by license only

Time Dependent Operator-split and Unsplit Schemes for One Dimensional Premixed Flames

G. GOYAL, P. J. PAUL, H. S. MUKUNDA and S. M. DESHPANDE *Department of Aerospace Engineering, Indian Institute of Science, Bangalore 560 012, India*

(Received March 31, 1987; in final form March 17, 1988)

Abstract—This paper is concerned with a study of an operator split scheme and unsplit scheme for the computation of adiabatic freely propagating one-dimensional premixed flames. The study uses unsteady method for both split and unsplit schemes employing implicit chemistry and explicit diffusion, a combination which is stable and convergent. Solution scheme is not sensitive to the initial starting estimate and provides steady state even with straight line profiles (far from steady state) in small number of time steps. Two systems H_2–Air and H_2–NO (involving complex nitrogen chemistry) are considered in present investigation. Careful comparison shows that the operator split approach is slightly superior than the unsplit when chemistry becomes complex. Comparison of computational times with those of existing steady and unsteady methods seems to suggest that the method employing implicit–explicit algorithm is very efficient and robust.

NOMENCLATURE

Cp_i	Specific heat of ith species at constant pressure (cal $gm^{-1} K^{-1}$)
Cp	$\Sigma_{i=1}^{NOS} Cp_i \cdot Y_i$, Specific heat of the mixture at constant pressure (cal $gm^{-1} K^{-1}$).
$\mathscr{D}_{i,j}$	Binary diffusion coefficient ($cm^2 s^{-1}$).
D_i	Diffusion coefficient of species i into a mixture ($cm^2 s^{-1}$).
h_i	$(h_i' + h_i^0)$, sum of the specific enthalpy and enthalpy of formation of the ith species (cal gm^{-1}).
H	Total enthalpy (cal gm^{-1}).
K	Thermal conductivity of the mixture (cal $cm^{-1} sec^{-1} K^{-1}$).
Max.	Means maximum.
Min.	Means minimum.
NOS	Number of species.
NOR	Number of Reactions
P	Pressure (Atmosphere).
R_a	Gas constant = 1.9872 cal $mole^{-1} K^{-1}$.
RR_i	Reaction rate term.
S_u	Flame speed (cm/sec).
T	Absolute temperature (K).
t	Time co-ordinate.
X_i	Mole fraction of species i.
x	Physical distance (cm).
Y_i	Mass fraction of ith species.

Greek Symbols

δ	Flame thickness.
Δh_i	Difference between the enthalpies of ith species before and after reactions.
ΔH^n	Difference in total enthalpies between two time levels.
$\Delta\Psi$	Cell size.

Δt	Time step.
ΔT	Temperature difference between two neighbouring cells.
ΔT^n	Difference in temperature between two time levels.
ΔY_i^n	Difference in mass fractions of i-th specie between two time levels.
ϕ	Equivalence ratio [((oxidiser/fuel) at stoichiometry)/(oxidiser/fuel)].
ϱ	Density of the mixture ($\mathrm{gm\,cm^{-3}}$).
Ψ	Distance co-ordinate $= \int \varrho dx \cdot (\mathrm{gm\,cm^{-2}})$.
τ	Non dimensional temperature.
$\dot{W}_i'''$	Volumetric production/consumption rate of chemical species ($\mathrm{gm\,cm^{-3}\,sec^{-1}}$).

Superscripts

n	Time level of integration.
$\overline{n+1}$	Notation for intermediate computational values in case of operator split scheme.
$n+1$	Time level of integration after one step.
$\simeq$	Equivalent to.
$-\infty$	Quantities at cold end.
$+\infty$	Quantities at hot end.

Subscripts

i	for species.
j	for species.
l	for cell.
u	for quantities at unburned end.
b	for quantities at burned end.

1 INTRODUCTION

Computation of one-dimensional laminar premixed flames with complex chemistry and realistic diffusion has been receiving considerable attention in recent times. GAMM Workshop (Warnatz, 1982) became a focal point for a concerted effort of several workers in this regard. The methods employed in the workshop are essentially time dependent and steady state techniques by several workers. Out of eight groups of the workshop, only one group solved the steady state conservation equations and rest solved the time-dependent conservation equations using either finite difference methods or finite element methods. In the earlier literature also, many of the authors have chosen time dependence approach for solving the one-dimensional premixed flame problem. One possible reason for the preference of unsteady approach may be that the approach to steady state is physically more realistic though not always computationally efficient. Further, the choice of initial profiles is more critical in the steady state methods compared to the unsteady methods. Only, one group (Smooke 1982, Smooke *et al.* 1982a, 1982b, 1983) in literature has successfully been applying steady state method using damped Newton technique claiming higher effeciency compared to the other existing methods. But recently, they too appeared to find difficulties in this method due to choice of the initial guess and shifted to a hybrid method with a combination of unsteady technique for initial integration and steady state technique for subsequent iterations (see Grcar *et al.* (1986)). While the concept

appears elegant, the superiority of their hybrid method over the other existing methods is rather premature to judge because the demonstration example shown by them is Formaldehyde-Oxygen system rather than H_2–Air system for which much is known in the literature.

Olsson and Andersson (1985) studied several test cases using an unsteady technique and indicated that their method was initially less efficient compared to steady state method (Smooke *et al.*, 1982b) and later (Andersson and Olsson (1986)) superior to it after a few modifications. Andersson and Olsson (1986) have presented a variety of details of computation to enable independent assessment of the power of their method. However, they use the measured temperature profile in their method. Methods based on this do not represent the true capability of the method which should be capable of solving the complex flame problem without using measured temperature profile. Also these methods always require experimentally measured values and have therefore limited use.

Devising an efficient and robust numerical scheme for obtaining the numerical solution of one dimensional premixed flame problem is a very challenging problem in the field of computation and as yet a totally satisfactory numerical scheme has not become available. The difficulty is mainly due to the difference in the physics behind the reaction and diffusion terms present in the governing equations. Because of this difference in behaviour many workers have thought it advisable to use an operator split scheme which allows different numerical schemes for the chemistry and diffusion. Operator splitting method originally developed by Yanenko (1971) has been applied to the computation of premixed laminar flame propagation by Dwyer and Sanders (1978), Otey (1978), Bhashyam *et al.* (1986) and others, and to the steady, laminar, diffusion flames by Kee and Miller (1977). Bhashyam (1984) has suggested after a brief review of various operator split schemes that an optimal combination of numerical schemes from the point of view of computational efficiency is still an open question.

Maximum benefit from the operator splitting approach can be had only when suitable schemes are used for the individual phenomena. One of the aims of the present work is to find out whether a noniterative implicit treatment of chemistry (instead of the Gear–Hindmarsh scheme used by Otey (1978)) and an explicit treatment of diffusion (instead of the probabilistic approach of Bhashyam *et al.* (1986)) leads to an optimal operator split scheme. We could use the above methods for the unsplit case also (*i.e.*, implicit treatment of chemistry together with explicit treatment of diffusion) and make a comparative study of the split and unsplit methods from the point of view of efficiency and robustness for a variety of problems involving complex chemistry. One of the important findings of the present investigation is that this combination of an explicit diffusion operator and an implicit chemistry operator yields a stable and convergent algorithm.

Present solution scheme is not sensitive to the starting guess, rough estimate of either flame thickness or flame speed helps in generating initial profiles (straight line) and the solution scheme carries them to the converged state in a relatively small number of time steps. Near equality of flame speeds based on most species with more than marginal mass fractions at one of the ends (hot or cold) and no change in flame speeds of major species for further successive time steps constitute the criterion for convergence to steady state. The computation time comparison of the present method and the methods developed by earlier workers is presented by using relative speeds of machines given by Dongarra (1985).

The split and unsplit schemes involving implicit and explicit treatments respectively for chemistry and diffusion have been applied to two problems namely, H_2–NO system and H_2–Air system. H_2–NO system has been chosen in particular as it

represents an oxidiser with same element as in air but involving entirely different kinetics. The kinetics of H_2–NO system is less investigated and prediction of H_2–NO flames has not been made in earlier literature.

A study on various ways of calculating diffusional velocities in trace diffusion approximation indicates little differences in flame speed in H_2–Air system and differences of the order of 4% in the case of H_2–NO system.

Larger cell size and time step may lead to problems of instability and inaccuracy in results (see Otey 1978). And smaller cell size and time step demand large computational times. The time step allowed has to be obtained by stability analysis which is quite complex for the present problem involving nonlinear source term due to reactions and multicomponent or trace diffusion model. The present study finds a way to select cell size and time step based on an empirical stability analysis. It has been found to yield accurate results with relatively small computational time.

2 THE EQUATIONS AND METHOD OF SOLUTION

2.1 *Operator Split Scheme*

The conservation equations in a laboratory fixed co-ordinates describing a laminar premixed flame can be written as:

$$\text{Species:} \qquad \partial Y_i/\partial t = -\partial J_i/\partial \Psi + \dot{W}_i'''/\varrho, \tag{1}$$

$$\text{Energy:} \qquad \partial H/\partial t = \partial/\partial\Psi[(K\varrho/Cp)(\partial H/\partial\Psi)] - \sum_{i=1}^{NOS} \partial/\partial\Psi[(J_i + K\varrho/Cp \cdot (\partial Y_i/\partial\Psi)) \cdot h_i] \tag{2}$$

Where ϱ is the mass density, K = thermal conductivity, Cp = specific heat of the mixture at constant pressure, H = total enthalpy of the mixture. Y_i, h_i, J_i and $\dot{W}_i'''$ are respectively the mass fraction, enthalpy, diffusive mass flux and reaction rate of the i-th species. The boundary conditions are that

$$\text{as} \qquad \Psi\left(= \int \varrho\, dx\right) \to -\infty : Y_i \to Y_i^{-\infty} \quad \text{and} \quad T \to T^{-\infty} \tag{3}$$

$$\text{and as} \qquad \Psi \to +\infty : Y_i \to Y_i^{+\infty} \quad \text{and} \quad T \to T^{+\infty} \tag{4}$$

The above conditions imply that

$$\partial Y_i/\partial\Psi \to 0 \quad \text{and} \quad \partial T/\partial\Psi \to 0 \quad \text{as} \quad \Psi \to +\infty$$

These gradient conditions are the actual boundary conditions applied at the hot boundary during computation. Sufficient number of cells are chosen so that at least five or six cells in the hot boundary region have equilibrium values of mass fractions and temperature.

Reaction and diffusion parts in the conservation equations are treated separately by the use of operator splitting. The energy equation is expressed in terms of total enthalpy and has no reaction term and hence the total enthalpy at a location is affected only by the diffusion operator. In the earlier work (Bhashyam *et al.*, 1986) the

reaction rate operator was treated numerically by using explicit Euler method. This resulted in the approach to steady state to be asymptotically oscillatory. To overcome this problem the chemical reaction part has been solved by using an implicit scheme called linear block method (Otey, 1978). Earlier, diffusion part was treated by a Gauss Markov process inspired unconditionally stable explicit scheme. Various numerical studies showed that one could use the FTCS (forward time and central space) scheme since the time step permitted by the chemistry operator was more restrictive than that allowed by the FTCS.

The method of solution for the operator split scheme is as follows:
The reaction rate term

$$dY_i/dt = \dot{W}_i'''/\varrho \tag{5}$$

is treated by

$$(Y_{il}^{\overline{n+1}} - Y_{il}^n)/\Delta t = (1/2)[(\dot{W}_i'''/\varrho)_l^{\overline{n+1}} + (\dot{W}_i'''/\varrho)_l^n] \tag{6}$$

where subscript i represents species and l the distance location. The subscript l will be omitted further in this paper.

After linearizing the term $(\dot{W}_i'''/\varrho)^{\overline{n+1}}$, Eq. (6) will appear as

$$[\partial(\dot{W}_i'''/\varrho)/\partial T]^n \cdot \Delta T^n + \sum_{j=1}^{\text{NOS}} [\partial(\dot{W}_i'''/\varrho)/\partial Y_j]^n \cdot \Delta Y_j^n - (2/\Delta t) \cdot \Delta Y_i^n = -2(\dot{W}_i'''/\varrho)^n \tag{7}$$

The total enthalpy remains constant during chemical reaction and hence

$$\sum_{i=1}^{\text{NOS}} h_i^n \cdot Y_i^n = \sum_{i=1}^{\text{NOS}} (h_i^n + \Delta h_i^n) \cdot (Y_i^n + \Delta Y_i^n) \tag{8}$$

Equation (8) after expanding and with the help of (5) give the following equation

$$\left[Cp^n + \sum_{i=1}^{\text{NOS}} Cp_i^n \cdot (\dot{W}_i'''/\varrho)^n \cdot \Delta t\right] \cdot \Delta T^n + \sum_{i=1}^{\text{NOS}} h_i^n \cdot \Delta Y_i^n = 0 \tag{9}$$

The Eqs. (7) and (9) can be written as

$$[A][U] = [B] \tag{10}$$

In the present method the Jacobian matrix $[A]$ is calculated at each mesh point after every time step. Here the Jacobian $[A]$ is (NOS + 1)X(NOS + 1) matrix unlike the block tridiagonal Jacobian matrix encountered by (Smooke, 1982). The above matrix system therefore can easily be solved by using Gaussian elimination method with partial pivoting. Once ΔT^n and ΔY_i^n are obtained, the quantities at $\overline{n+1}$th time step are obtained from $T^{\overline{n+1}} = T^n + \Delta T^n$ and $Y_i^{\overline{n+1}} = Y_i^n + \Delta Y_i^n$. Knowing $T^{\overline{n+1}}$ and $Y_i^{\overline{n+1}}$ after reaction, the diffusion operation is performed on these profiles for the same time step to get T^{n+1} and Y_i^{n+1}. This completes the computation for one step.

As mentioned before both multicomponent model and trace diffusion model have been used to calculate the diffusive fluxes. The multicomponent diffusion model used

here is similar to the Method II of Coffee and Heimerl (1981) in which only one term in the Sonine polynomial expansion is taken (after rearrangement it gives Stefan–Maxwell equations). These Stefan–Maxwell equations along with the constraint $\Sigma_{i=1}^{NOS} Y_i V_i = 0$ make an NXN matrix system to be solved for N unknown diffusion velocities. While using the trace diffusion model a correction in diffusion velocities is performed according to the scheme proposed by Oran and Boris (1981). Diffusive mass flux J_i in this case is written as follows:

$$J_i = -[D_i \varrho^2 \partial Y_i/\partial \Psi - Y_i \sum_{j=1}^{NOS} D_j \varrho^2 (\partial Y_j/\partial \Psi)]$$

Transport properties are calculated using relations of Brokaw (1961) by using the Lennard–Jones potential parameters given by Warnatz (1978b). Thermal diffusion has not been included in the present calculations.

2.2 *The Unsplit Scheme*

In the unsplit scheme diffusion and chemistry terms are considered together. Species conservation Eqs. (1) can be written in the following differenced form, treating the chemistry in implicit manner.

$$\Delta Y_i^n/\Delta t = -\Delta J_i/\Delta \Psi + (1/2) \cdot [(\dot{W}_i'''/\varrho)^{n+1} + (\dot{W}_i'''/\varrho)^n] \tag{11}$$

Linearizing $(\dot{W}_i'''/\varrho)^{n+1}$, the above equation is written as

$$[\partial(\dot{W}_i'''/\varrho)/\partial T]^n \cdot \Delta T^n + \sum_{j=1}^{NOS} [(\partial(\dot{W}_i'''/\varrho)/\partial Y_j) \cdot \Delta Y_j]^n - (2/\Delta t) \cdot \Delta Y_i^n$$

$$= -2[\mathrm{DIFF}_i + (\dot{W}_i'''/\varrho)]^n \tag{12}$$

Where $\mathrm{DIFF}_i = -\Delta J_i/\Delta \Psi$
Similarly, the energy Eq. (2) can be written as

$$(\Delta t) \cdot \left[\partial/\partial \Psi[K\varrho/Cp \cdot (\partial H/\partial \Psi)] - \sum_{j=1}^{NOS} \partial/\partial \Psi[(J_j + K\varrho/Cp \cdot (\partial Y_j/\partial \Psi)) \cdot h_j]\right]^n$$

$$= \Delta H^n = \sum_{i=1}^{NOS} (h_i^n + \Delta h_i^n) \cdot (Y_i^n + \Delta Y_i^n) - \sum_{i=1}^{NOS} h_i^n Y_i^n \tag{13}$$

After expanding the r.h.s. term and by using Eq. (1), we can write the energy equation in the following form

$$\left[Cp^n + \sum_{i=1}^{NOS} Cp_i^n[\mathrm{DIFF}_i + \dot{W}_i'''/\varrho]^n \cdot \Delta t\right]\Delta T^n + h_1^n \Delta Y_1^n + h_2^n \Delta Y_2^n$$

$$+ - - - h_{NOS}^n \Delta Y_{NOS}^n = \Delta H^n \tag{14}$$

The Jacobian remains block diagonal as in the split scheme and hence can be solved cell by cell. In the unsplit scheme profiles are calculated from nth step to $n + 1$th step without any intermediate step.

2.3 *Split vs Unsplit Schemes*

In order to examine if the operation of splitting causes any truncation error, the species conservation equation was subjected to the following analysis.

The analysis begins by setting

$$\overline{Y_i^{n+1}} = Y_i^n + (RR_i) \cdot \Delta t \quad \text{from} \quad dY_i/dt = RR_i$$

in the equation,

$$(Y_i^{n+1} - \overline{Y_i^{n+1}})/\Delta t = \partial/\partial\Psi[D_i\varrho^2 \cdot (\partial \overline{Y_i^{n+1}}/\partial\Psi)]$$

leading to

$$\partial Y_i/\partial t = \partial/\partial\Psi[D_i\varrho^2 \cdot (\partial Y_i^n/\partial\Psi)] + RR_i + (\Delta t) \cdot \partial/\partial\Psi[D_i\varrho^2 \cdot (\partial RR_i/\partial\Psi)] \tag{15}$$

Due to splitting the term $(\Delta t) \cdot \partial/\partial\Psi[D_i\varrho^2 \cdot (\partial RR_i/\partial\Psi)]$ is introduced, a feature absent in the unsplit scheme. This term represents the artificial diffusion of reaction rate term. Effect of this term is discussed later.

3 COMPUTATIONAL PROCEDURE

3.1 *Cell Size and Time Step Selection*

For an entirely new flame system it is difficult to choose the appropriate cell size and time step at the beginning of the computation. But knowing the class of the flame and approximate knowledge about its flame speed with estimates of K/Cp and ϱ_u, the approximate thickness of the flame can be calculated using the formula $\delta = C \cdot (K/Cp) \cdot [1/(\varrho_u \cdot S_u)]$ where C is some dimensionless constant and is identified from a known case. Once a reasonable idea about flame thickness is obtained, the flame can be adequately resolved by choosing $\Delta\Psi = \varrho_{av.}\delta/(\text{Number of cells})$ where the number of cells is generally 30 to 40. The time step can then be obtained from the stability criterion $\Delta t \leqslant 0.5(\Delta\Psi)^2/(D_i\varrho^2)_{max}$ where $(D_i\varrho^2)_{max}$ is the maximum value of $D_i\varrho^2$ in the entire field for all the species. The above criterion is based on the stability analysis of FTCS applied to the diffusion term only. As mentioned previously the stability study for the full equation is in general very complex. It has been found from the calculations performed that $\Delta\Psi$ and Δt so determined are good enough for starting the computations. As the computations proceed we progressively tune $\Delta\Psi$ and Δt in such a way that they lead to a maximum temperature difference between two adjacent cells not exceedingly 8 to 12% of the adiabatic flame temperature at converged state. For this, a trial run upto 20 time steps with the chosen values of $\Delta\Psi$ and Δt will indicate if the maximum temperature difference between any two adjacent cells will be about 8–12% of the adiabatic flame temperature, if not then, suitable corrections to $\Delta\Psi$ and Δt can be obtained in additional one or two trial runs of twenty steps at most (which will cost just 20% of the total CPU time at most). When some reasonable estimate of the flame thickness or flame speed is known, number of trials reduces and hence the CPU time.

3.2 *Initial conditions*

It is stated by Smooke *et al.* (1982, 1983) that the steady state method calls for initial profiles not too far from the steady state. They used measured temperature profile for

the initial iterations thereby making the method dependent on experimental results. Unsteady methods do not call for such a dependence on experimental information.

In the present work a very simple method has been developed to generate initial profiles. The idea is to use the iso enthalpy concept and element conservation throughout the field.

First we take a straight line for temperature which is smoothened at the hot and cold ends. Mass fractions profiles for radical species are calculated using

$$Y_i = Y_i^{-\infty} + (Y_i^{+\infty} - Y_i^{-\infty}) \cdot \tau \tag{16}$$

$$\text{where} \quad \tau = (T - T^{-\infty})/(T^{+\infty} - T^{-\infty})$$

Mass fraction profiles for major species are calculated by solving the following linear equations of constant enthalpy and elemental conservation

$$H^{-\infty} = \sum_{i=1}^{\text{NOS}} h_i \cdot Y_i \tag{17}$$

$$Ye_i^{-\infty} = \sum_{j=1}^{\text{NOS}} Y_j \cdot a_{i,j} \tag{18}$$

where Ye_i is the mass fraction of element i in the mixture.
$a_{i,j}$ is the mass fraction of element i in specie j.

Equations (17) and (18) form a set of simultaneous linear algebraic equations to be solved after noting that the values of radical species are known from Eq. (16).

The use of iso-enthalpy and elemental conservation all through the field in the beginning of the computation has been made even though they will change due to effects of non unity Lewis number, because departures from the state of constancy is not large and this happens to be a good starting point.

Generation of initial profiles in the above manner is a simple task requiring only a small amount of calculations and is automated in the code itself.

3.3 *Computation Without Sizing*

For this purpose the physical space is divided in to 100 cells. In the beginning of the integration around 40 cells are in the computational domain, out of which 10 contain adiabatic flame temperature and equilibrium composition (calculated from NASA-SP-273 (Gordon and Mcbride, 1971) program) serving the hot boundary condition. About 30 cells are filled with values given by initial profiles described earlier. A constant cell size (in Ψ plane) and time step are selected as described in Section 3.1.

During the initial integration profiles move towards both hot and cold boundaries. Provision has been made to push automatically a few hot boundary cells if in the 3rd cell from hot end, flame temperature changes by ± 0.5 K. Towards the cold boundary, enough cells are put in for movement of profiles. After sufficient integration (200 time steps) movement of profiles generally occurs towards cold boundary, thereby leaving many number of cells in hot boundary inactive. In this case unnecessary calculations are eliminated by sizing procedure described below.

3.4 *Computation With Sizing*

In sizing procedure extra hot boundary cells are eliminated by an automatic check in the code at every 10 steps in which the magnitude of the heat release rate in all cells are compared with maximum value of heat release rate. The cells which contain heat release rate less than a thousandth of the maximum heat release rate are neglected. At every sizing check two new cells containing equilibrium values are introduced at the hot end.

Towards the cold boundary the chemistry part is skipped in those cells which contain the heat release rate less than ten millionth of maximum heat release rate. In these cells (which range from 8 to 15) only diffusion is performed. Transport properties for these cells are calculated at every 10 time steps. Sizing treatment towards both hot and cold boundary reduces computational time by about a factor of two and the results are within 1% with that of the results obtained without sizing.

4 RESULTS AND DISCUSSION

The results of two systems, H_2–Air and H_2–NO, are presented here. A fairly simple H_2–Air flame (8 species, 11 reversible reactions, $P = 1$ Atmosphere, $\phi = 1$) uses the chemical kinetics mechanism suggested as a test bed in GAMM Workshop (Warnatz, 1982). In the Table II of summary paper of Warnatz (1982), reaction (6) $OH + O + M \rightarrow HO_2 + M$ was stated to be put in by misprint instead of $H + OH + M \rightarrow H_2O + M$. Smooke *et al.*, (1982a) in the same workshop have given the correct reaction mechanism. But Dasch and Blint (1983) have not corrected the mistake. We treat the corrected mechanism.

H_2–NO system (10 species, 10 reversible reactions, $P = 1$ Atmosphere, $\phi = 1$) uses the kinetic mechanism which is reduced compared to the full set given by Flower *et al.* (1974). Table I gives the reaction mechanism and the reaction constants used in present work. Both H_2–Air and H_2–NO contain the same elements H–N–O, but kinetics of the two systems are widely different. H_2–NO system is more complex than H_2–Air due to its involvement of Nitrogen element as important participant in reactions.

The calculations are considered to be converged when flame speeds of major species do not change for further successive time steps and also when flame speeds based on most species with more than marginal mass fractions at one of the ends (hot or cold) become nearly equal. To see how much change will occur if the code is run for very

TABLE I

Hydrogen–Nitric oxide reaction mechanism. $k_r = A_r T^{B_r} e^{-E_r/RT}$ (units are moles, cm^3, sec)

r	Reaction	A_r	B_r	E_r
1	$H + NO = N + OH$	1.34×10^{14}	0.0	49 200.0
2	$O + NO = N + O_2$	2.36×10^{9}	1.0	38 640.0
3	$O + N_2 = N + NO$	7.00×10^{13}	0.0	75 500.0
4	$NO + H + M = HNO + M$	5.40×10^{15}	0.0	−596.0
5	$HNO + H = H_2 + NO$	3.00×10^{11}	0.5	2 385.0
6	$HNO + OH = H_2O + NO$	3.00×10^{12}	0.5	2 385.0
7	$H_2 + O = H + OH$	1.80×10^{10}	1.0	8 900.0
8	$O_2 + H = O + OH$	2.20×10^{14}	0.0	16 800.0
9	$H_2O + H = OH + H_2$	9.30×10^{13}	0.0	20 360.0
10	$H_2O + O = OH + OH$	6.80×10^{13}	0.0	18 360.0

TABLE II
Verification of the achievement of steady state. H_2–Air System (8 species and 11 reversible reactions) (Using Multicomponent Diffusion Mode, split scheme and sizing)

Step No.	Su_{O_2}	Su_{H_2}	Su_{H_2O}	$Su_{By\ En.\ Eq.}$
350	202.8	203.2	202.6	203.1
1650	202.5	203.4	202.3	203.4

H_2–NO System (10 species and 10 reversible reactions) (Using Trace Diffusion Model, split scheme and sizing)

Step No.	Su_{O_2}	Su_{H_2}	Su_{H_2O}	Su_{N_2}	Su_{NO}	$Su_{By\ En.\ Eq.}$
500	248	251	251	250	251	251
1650	249	250	251	250	251	250

large number of time steps after achieving the steady state, we ran the code for both H_2–Air and H_2–NO systems up to 1650th steps, on comparing the flame speeds with that at 350th step (in case of H_2–Air) and 500th step (in case of H_2–NO) only negligible difference ($< 0.5\%$) was noticed (see Table II). This shows that the steady state is achieved at around 350th step (H_2–Air) and 500th step (H_2–NO).

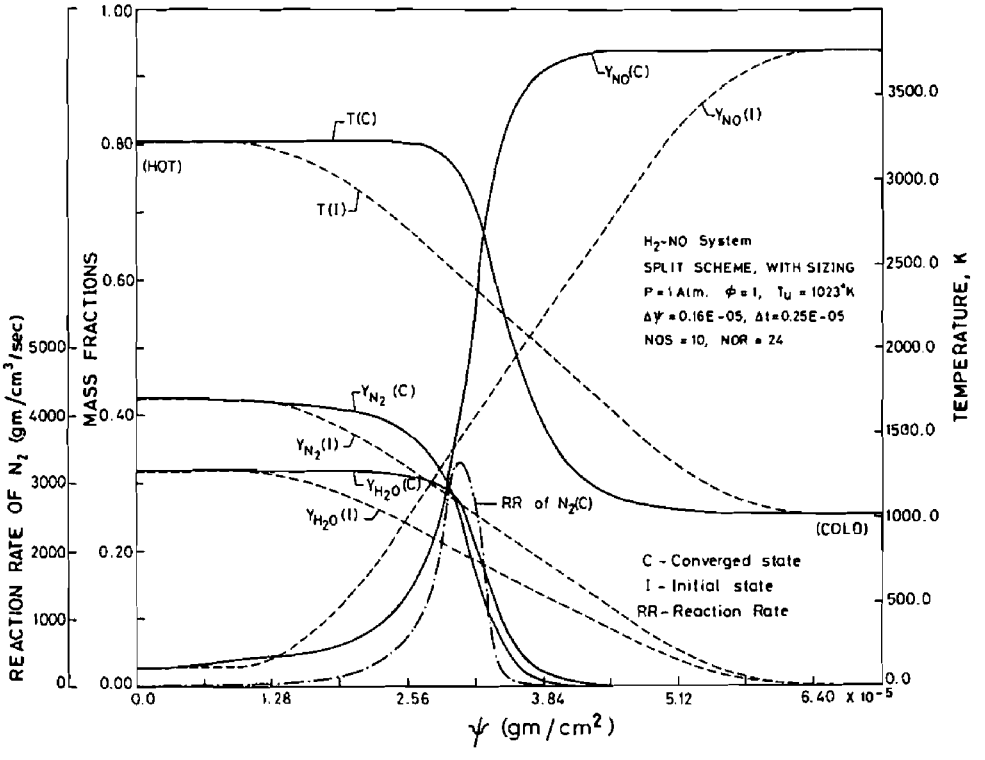

FIGURE 1 Plot of mass fraction of H_2O, N_2, NO species and temperature with Ψ-co-ordinate at initial and converged state.

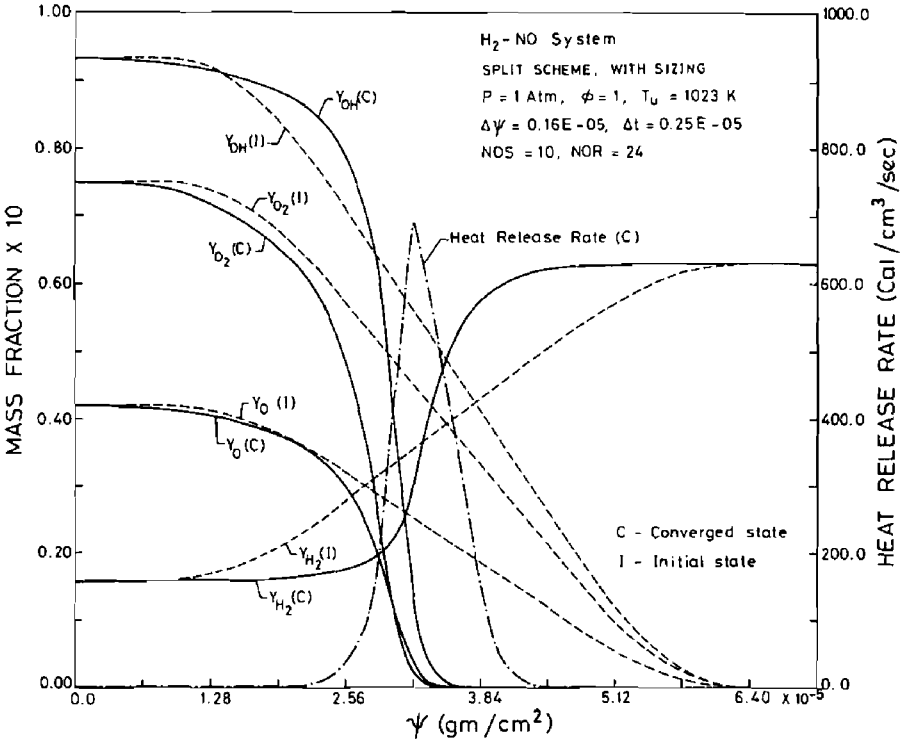

FIGURE 2 Plot of mass fraction of O_2, O, H, OH species at initial and converged state and heat release rate with Ψ co-ordinate.

For both H_2–Air and H_2–NO systems initial profiles were generated in the manner as described in Section 3.2. Figures 1–3 show the mass fraction profiles of H_2–NO system against Ψ co-ordinate at initial and steady state. In Figure 1 profiles of mass fraction of H_2O, N_2 and NO, temperature and reaction rate of specie N_2 are plotted. The reaction rate is included to indicate the region of importance in the converged state. Figure 2 contains the profiles of mass fraction of O_2, O, H_2 and OH and heat release rate. Mass fraction profiles of species N, H and HNO are plotted in Figure 3. Even though the final steady state profiles are thinner than the initial profiles, during initial integration profiles moved simultaneously both towards hot and cold boundary. For the results of Figures 1–3, the steady state profiles are obtained after using the sizing procedure. Figures 1–3 show that the initial straight line profiles (far from steady state) seem to be satisfactory and the solution scheme carries them to the smooth shape at converged state. Furthermore, robustness of the method is seen from Figure 3 where near zero values of mass fractions in the initial profiles of HNO and N do not seem to matter in carrying them to significant values at steady state. Figure 1 shows the profile of reaction rate of specie N_2 and Figure 2 the profile of heat release rate at converged state. It is apparent from these Figures (1–3) that around 15 cells are in active flame region. At converged state 45 cells are in computational domain with cell size $\Delta\Psi = 0.16E\text{-}05$ and time step $\Delta t = 0.25E\text{-}05$, 500 steps were required for computation using split scheme.

Operator split and unsplit schemes have been used in the present study. Both the schemes gave matching flame speeds for number of species within 2% error band in

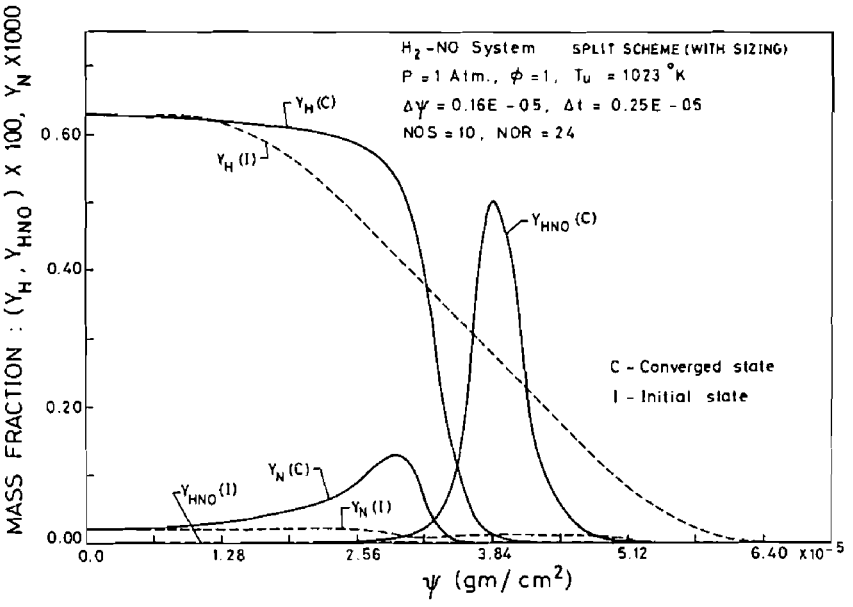

FIGURE 3 Plot of mass fraction of H, N and HNO species with Ψ co-ordinate at initial and converged state.

TABLE III

Split vs. Unsplit. H_2–Air System (8 Species, 11 Reversible Reactions) (Using Multicomponent Diffusion Model and sizing) $\Delta\Psi$ = 0.2E-05, Δt = 0.15E-05, No. of steps = 350

Scheme	Su_{O_2} cm/sec	Su_{H_2}	Su_{H_2O}	$Su_{By\,En.\,Eq.}$	CPU time on DEC 1090
Split	202.8	203.2	202.6	203.1	760s
Unsplit	201.0	200.5	200.8	199.8	760s

H_2–NO System (10 Species, 10 Reversible Reactions) (Using Trace Diffusion Model and sizing) $\Delta\Psi$ = 0.16E-05, Δt = 0.25E-05, No. of Steps = 500

Scheme	Su_{O_2} cm/sec	Su_{H_2}	Su_{H_2O}	Su_{N_2}	Su_{NO}	$Su_{By\,En.\,Eq.}$	CPU time on DEC 1090
Split	248	251	251	250	251	251	1620s
Unsplit	250	248	247	248	249	248	1800s

both H_2–Air and H_2–NO flame (see Table III). In case of H_2–Air system CPU time was same for both split and unsplit schemes for the same number of steps while H_2–NO system showed 11% increase in CPU time from split to unsplit scheme for the same number of time steps. On closer examination of the results, it was found that the split scheme was allowing larger time step (*i.e.*, time step fractioning was less) compared to the unsplit scheme particularly in the initial stages of computations and hence split scheme seemed more efficient than unsplit scheme in the cases of complex chemistry. A provision was made in the program to integrate the chemical kinetic equation using fractional time steps if the normal time step produced negative mass

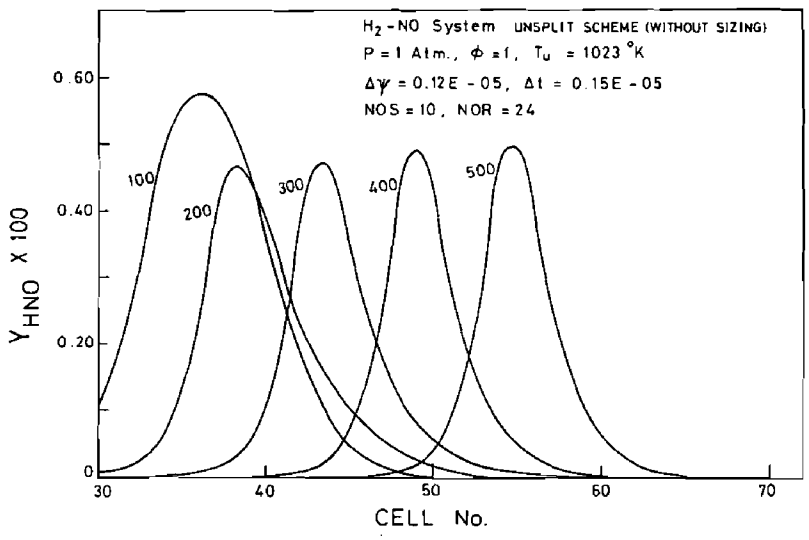

FIGURE 4 PLot of mass fraction of HNO with cell No. at different time steps.

fractions. This problem could not be overcome by corrective iterations and fractional time step was necessary.

It has been discussed earlier in this paper that split scheme introduces a term called artificial diffusion of reaction rate term. The effect of this error term is that, the flame speeds computed for various species do not become equal even after about 250–300 steps in case of H_2–Air system and 400–450 steps in case of H_2–NO system. In order to reduce this error the computations have to be made at much lower Δt since the error is proportional to Δt^2. The computations were made with normal Δt until stationary profiles are obtained and then Δt was reduced gradually to about one hundredth of its initial value in about hundred steps. This problem is not encountered in unsplit scheme and equal flame speeds were obtained with normal Δt.

Flame speeds of the radical species (*e.g.*, N and HNO in case of H_2–NO system) which have near zero values at hot and cold end do not match with the flame speeds of other species. For such species flame speed can be found by the movement of profiles on grids with time.

Figure 4 shows the plot of mass fraction of HNO specie with cell number at different time steps. Taking unsplit scheme with $\Delta\psi$ = 0.12E-05 and Δt = 0.15E-05 flame speed of HNO specie has been found from the graph itself. Taking the distance between the peak of 400 and 500 time steps' profiles as 2.88 cm and ϱ_u = 0.1097E-03 g/cm^3, we get S_u of HNO specie as 241 cm/sec, which is 8 cm/sec less than the converged value which is achieved around 850th time step taking the small cell size and time step. For the results of Figure 4, sizing procedure is not performed. Here profiles can be seen moving on the grids with the same flame speed after sufficient integration.

In Table IV the flame speeds of various species and by energy equation are presented for both H_2–Air and H_2–NO systems. Sizing procedure has been found to save the computational time by a factor of 2 within 1% of the results obtained without sizing. Using the sizing procedure the movement of profiles on grids cannot be seen as is seen in Figure 4 where sizing procedure has not been used.

An interesting study (different from the one which was done by Coffee and Heimerl (1981)) about various diffusion velocity models in case of trace diffusion approximation

TABLE IV
Sizing vs. Unsizing. H_2–Air System (8 Species, 11 Reversible Reactions) (Using Multicomponent Diffusion Model and split scheme)

Procedure	Su_{O_2} cm/sec	Su_{H_2}	Su_{H_2O}	$Su_{By\ En.\ Eq.}$	CPU time on DEC 1090
Without sizing	203.3	202.9	203.2	202.5	1450 s
With sizing	202.8	203.2	202.6	203.1	760 s

H_2–NO System (10 Species, 10 Reversible Reactions) (Using Trace Diffusion Model and split scheme)

Procedure	Su_{O_2} cm/sec	Su_{H_2}	Su_{H_2O}	Su_{N_2}	Su_{NO}	$Su_{By\ En.\ Eq.}$	CPU time on DEC 1090
Without sizing	251	250	250	249	250	251	3560 s
With sizing	248	251	251	250	251	251	1620 s

was done and results were compared with that of the multicomponent diffusion model. Table V shows the various diffusion models used and the flame speed calculated using these models for both H_2–Air and H_2–NO systems. Model A uses multicomponent diffusion, model B uses trace diffusion approximation in the form suggested by Curtiss–Hirschfelder (1949), model C is derived from model B assuming average molecular weight as constant (used by Warnatz (1978a)), model D is same as model C except a change of $1\text{-}X_i$ instead of $1\text{-}Y_i$. Model B and D are same for a typical case of binary mixture. It has been observed in the present study that in almost all cases model D gives the results close to model A. Table V shows that in the case of H_2–Air system all the four models produce almost the same flame speeds (less than 1% compared to model A); but in case of H_2–NO system the differences are of the order of 4%. Result of model D was found to be closest to that of model A. Model D with correction in diffusion velocities due to Oran and Boris (1981) has been found to be a good substitute of multicomponent diffusion model and has been used in the present work.

Comparison of CPU times shows that the mutlicomponent diffusion model needs 15% more CPU time compared to trace diffusion approximation. Thus the extra time budget needed to get accurate results for any system does not seem very significant.

Several runs were made in order to examine the effect of cell size and time step on the solution; and the results are summarised in Table VI. It can be seen from this table that the flame speed becomes independent of cell size when the maximum temperature difference between any two adjacent cells (at converged state) is less than 12% of the flame temperature for both H_2–Air and H_2–NO systems. With larger cell sizes (see sets 1(b), 2(b), 3(b) and 4(b) of Table VI); the calculated flame speed decreases with increase in cell size—an observation made by many earlier workers (Reitz, 1980 and Warnatz, 1982) on unsteady methods. The increase in calculated flame speeds with increase in cell size obtained by Smooke *et al.*, (1982a) is due to the artificial diffusivity introduced by the upwind differencing of the convection term.

The results of several calculations are shown in Figure 5 which displays various regions in the $(\Delta\Psi, \Delta t)$ plane. The Courant stability condition $\Delta t = 0.5(\Delta\Psi)^2/(D_i\varrho^2)_{max}$ for FTCS scheme gives a parabola in the $(\Delta\psi, \Delta t)$ plane. It is the usual practice to choose $\Delta t = (0.8) \cdot \Delta t_{crit} = 0.4(\Delta\Psi)^2/(D_i\varrho^2)_{max}$ giving another parabola shown in the Figure 5. Obviously, only those of values of $\Delta\Psi$, Δt which fall in the stability region are allowed. Even within this region all combinations of $\Delta\Psi$, Δt are

TABLE V
Various diffusion models

	Models	H_2–Air System		H_2–NO System	
		Flame speed cm/sec	CPU time on DEC 1090 sec	Flame speed cm/sec	CPU time on DEC 1090 sec
[I] (A)	Multicomponent Diffusion (One Term Sonine Polynomial Expansion)	203	760	253	1860
[II]	Trace Diffusion Model				
	$\text{Flux} = \varrho \cdot \left[V_i' - \sum_{j=1}^{\text{NOS}} V_j' Y_j \right] \cdot Y_i$				
(B)	$V_i' = -\left[X_i^{-1} \cdot \left[(1 - Y_i) \Big/ \left(\sum_{j=1}^{\text{NOS}} X_j / \mathscr{D}_{ij} \right) \right] \cdot dX_i/dx \right]$	204	650	260	1620
(C)	$V_i' = -\left[Y_i^{-1} \cdot \left[(1 - Y_i) \Big/ \left(\sum_{j=1}^{\text{NOS}} X_j / \mathscr{D}_{ij} \right) \right] \cdot dY_i/dx \right]$	205	650	263	1620
(D)	$V_i' = -\left[Y_i^{-1} \cdot \left[(1 - X_i) \Big/ \left(\sum_{j=1}^{\text{NOS}} X_j / \mathscr{D}_{ij} \right) \right] \cdot dY_i/dx \right]$	202	650	250	1620

TABLE VI
Various cell sizes and time steps sets (Using Split Scheme with Trace Diffusion Model)

Set	System	$T_b(K)$	$(\Delta T)_{max}$ (converged) K	$\Delta\Psi$	Δt	Computed S_u cm/sec	$(\Delta T)_{max}$ (step 1) K	$(\Delta T)_{max}$ (step 10) K	$(\Delta T)_{max}$ (step 20) K
	H_2–Air								
1(a).	$P = 1, \phi = 1, T_u = 298$ K	2378	–	0.400E-5	0.6000E-5	–	83.5	347.5	431.6
1(b).	$P = 1, \phi = 1, T_u = 298$ K	2378	496	0.400E-5	0.1500E-5	189.0	83.5	137.1	241.2
2(a).	$P = 1, \phi = 1, T_u = 298$ K	2378	–	0.350E-5	0.4603E-5	–	83.5	285.5	385.4
2(b).	$P = 1, \phi = 1, T_u = 298$ K	2378	452	0.350E-5	0.1500E-5	194.0	83.5	136.2	231.0
3(a).	$P = 1, \phi = 1, T_u = 298$ K	2378	–	0.300E-5	0.3380E-5	–	83.5	220.1	312.0
3(b).	$P = 1, \phi = 1, T_u = 298$ K	2378	386	0.300E-5	0.1500E-5	197.0	83.5	134.8	216.4
4(a).	$P = 1, \phi = 1, T_u = 298$ K	2378	–	0.250E-5	0.2349E-5	–	83.5	169.0	239.2
4(b).	$P = 1, \phi = 1, T_u = 298$ K	2378	319	0.250E-5	0.1500E-5	199.0	83.5	132.5	196.5
5.	$P = 1, \phi = 1, T_u = 298$ K	2378	256	0.200E-5	0.1500E-5	202.0	83.5	128.4	179.4
6.	$P = 1, \phi = 1, T_u = 298$ K	2378	239	0.186E-5	0.1300E-5	202.0	83.5	116.9	165.0
7.	$P = 1, \phi = 1, T_u = 298$ K	2378	194	0.150E-5	0.8450E-6	201.0	83.5	97.7	129.1
8.	$P = 1, \phi = 1, T_u = 298$ K	2378	129	0.100E-5	0.3750E-6	200.5	83.5	85.1	93.9
9.	$P = 1, \phi = 1, T_u = 298$ K	2378	-	0.500E-6	0.9375E-7	-	83.5	85.8	83.9
	H_2–NO								
10.	$P = 1, \phi = 1, T_u = 1023$ K	3216	355	0.160E-5	0.2500E-5	251.0	87.8	158.5	188.1
11.	$P = 1, \phi = 1, T_u = 1023$ K	3216	322	0.145E-5	0.2000E-5	250.0	87.8	153.8	167.8
12.	$P = 1, \phi = 1, T_u = 1023$ K	3216	269	0.120E-5	0.1500E-5	249.0	87.8	147.2	153.5

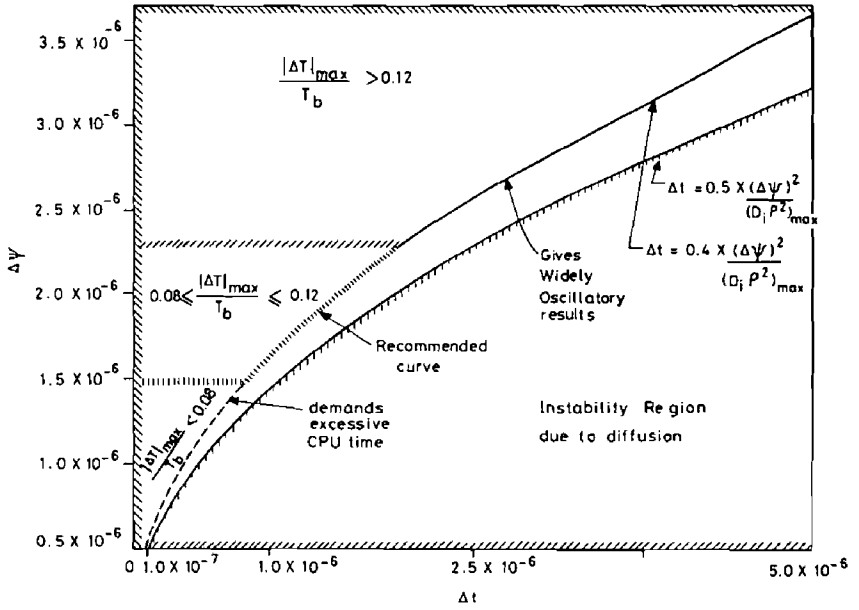

FIGURE 5 Empirical stability studies.

not permissible. For example, widely oscillatory behaviour will result if values of $\Delta\Psi$ chosen are such that $(\Delta T)_{max}$ (i.e. maximum temperature difference between two neighbouring cells) is more than 12% of the flame temperature at converged state. Alternatively, values of $\Delta\Psi$ leading to $(\Delta T)_{max}$ lower than 8% of the flame temperature will result in extremely slow convergence with a very marginal improvement of the accuracy. The region of convergence has been found to be a section of the curve $\Delta t = 0.4(\Delta\Psi)^2/(D_i\varrho^2)_{max}$ shown in Figure 5. For this section of curve $(\Delta T)_{max}$ falls within 8% to 12% of the flame temperature at converged state. It is interesting to observe that the cell sizes chosen by others (Lund, 1978; many participant of GAMM Workshop, see B. GRID SYSTEM of Table 3 of summary paper by Warnatz, 1982) even with adaptive grids fall in the same range that is 8 to 12% of the flame temperature.

In case of H_2–NO system, flame temperature is 3216 K, and 8 to 12% of this temperature is 257 K to 386 K. Sets 10, 11 and 12 give the maximum ΔT at converged state within this range and flame speed given by these sets is within 1% of each other. Sets 10 and 11 give convergence faster than set 12 due to the reason that sets 10 and 11 have bigger time step compared to set 12. It is apparent from Table VI that after examining the ΔT_{max} within twenty time steps, one can choose the proper set of cell size and time step.

Figure 6 shows the plots of S_u (by energy equation) against time steps (up to 50 steps) for various cell sizes and time steps values (set 1(a), 3(a) and 5 to 9 of Table VI). Oscillations produced by the use of large time step in set 1(a) and set 3(a) of Table VI can be seen in the Figure 6. Sets 5, 6 and 7 do not produce oscillations after a few steps. In these cases convergence is also smooth. Present study indicates that these sets are quite satisfactory on the basis of accuracy and CPU time expenditure. Set 8 takes more CPU time to give the same kind of accuracy, set 9 is very slow and has not been run till steady state.

It is possible to take much larger cell size and time step than indicated in the present study if measured temperature profile is used instead of solving energy equation.

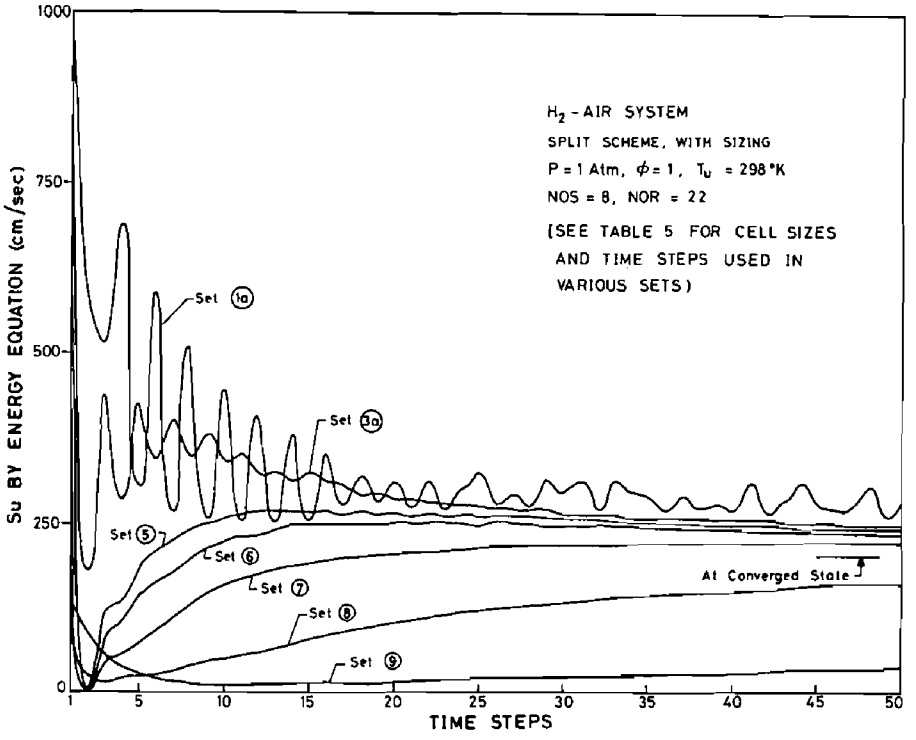

FIGURE 6 S_u (By Energy Equation) Vs. time steps with various cell sizes.

When energy equation is being solved along with species equations some of the eigenvalues of the Jacobian matrix becomes positive giving restriction on time step. If energy equation is not solved and measured temperature profile is used then all eigenvalues are negative implying no time step restriction. Andersson and Olsson (1986) use this fact in their grid sequencing procedure. They start with very coarse grid taking 5–10 points and go on refining it by introducing more number of points manually.

Table VII shows the computed flame speed S_u at various equivalence ratios (from lean to rich mixture) for H_2–Air system. Time steps needed for convergence is also

TABLE VII

Flame speed S_u at various equivalence ratio (Using trace diffusion model). H_2–Air System*: P = 1 Atm, T_u = 298 K

Sl. No.	Eq. Ratio ϕ	$\Delta\Psi$	Δt	Su cm/s	No. of Time Steps needed for convergence
1.	0.25	0.7500E-05	0.1400E-04	13.6	475
2.	0.50	0.2000E-05	0.1500E-05	78.0	400
3.	1.00	0.2000E-05	0.1500E-05	202.0	350
4.	1.50	0.1600E-05	0.9000E-06	252.0	360
5.	1.75	0.1659E-05	0.8400E-06	255.0	375
6.	5.62	0.2500E-05	0.9453E-05	95.0	400
7.	7.23	0.3000E-05	0.1769E-04	55.0	450

*Using the reaction kinetic mechanism same as given in GAMM Workshop for the test problem B (Warnatz, 1982).

TABLE VIII
CPU times comparison. H_2–Air system: $P = 1$ Atm, $\phi = 1$

Authors	Smooke	Warnatz	Reitz	Theis/Peters	Present
Computer	CRAY-1S	IBM 370/168	IBM 4341	CYBER 175	DEC-1090
MFLOPS†	12*	1.2*	0.22**	1.8*	0.25**
No. of cells used	53	36	51	40	50
No. of time steps	-	$\simeq 1000$	$\simeq 1000$	$\simeq 500$	$\simeq 350$
Total CPU time on Authors' Computer	55 s	400 s	3500 s	640 s	760 s
Equivalent CPU time on CRAY-1S	55 s	40 s	64 s	96 s	16 s
CPU time per time step	-	0.04 s	0.064 s	0.19 s	0.046 s
CPU time per time step per mesh point	-	1.1×10^{-3} s	1.3×10^{-3} s	4.8×10^{-3} s	0.9×10^{-3} s

†Dongarra (1985).
*Speed for full precision (64 bit) calculations.
**Speed for single precision calculations.

shown in this table. From here, it is evident that present method is capable of solving any flame (lean to rich) with at the most 35% extra time in the worst case.

Having shown the robustness of the method, it is appropriate to examine the computational efficiency of the method. The present method requires the calculations of one function and Jacobian evaluation each per step. Since the resulting matrix is block diagonal, rather than block tridiagonal as in the fully implicit formulation of various workers, the solution of the matrix equation should be comparatively faster. In Table VIII, the computational times of various workers' methods, the number of time steps needed for convergence and the number of mesh points (data taken from Warnatz (1982)) are presented along with those of the present method. For the sake of comparison the equivalent time in CRAY-1S is also provided, calculated from the comparative speeds of machines given by Dongarra (1985) obtained by solving a set of linear algebraic equations on various machines. It can be seen that the CPU time per time step per mesh point is roughly equal in most of the methods including the present one. However, the present method converges in about 350 steps (H_2–Air) compared to other methods which take large number of time steps. It is unlikely that this is due to the choice of initial profiles, since the choice of initial estimate was fairly crude as was explained earlier. We believe that choice of appropriate methods for the two physical processes, *viz.* diffusion and chemical reaction, resulted in optimum Δt and attainment of convergence in relatively small number of time steps.

One interesting point of Table VIII is that steady state method developed by Smooke (1982) has not been any time faster than the unsteady state methods, (even during 1982 Warnatz's method was faster than Smooke's). Recently, Andersson and Olsson (1986) also showed that their computational times were a factor 2–3 shorter than the computational times taken by the steady state method developed by Smooke (1982) for the same kind of problem.

4.1 *H_2–Air Flame*

Figures 7 to 9 contain a comparison between the present results and the corresponding ones from Smooke *et al.* (1982b). Except minor differences the agreement between both the results is excellent. About flame speed, there is some confusion in reporting the results of Smooke in GAMM Workshop. Smooke *et al.* (1982a, 1982b) indicate

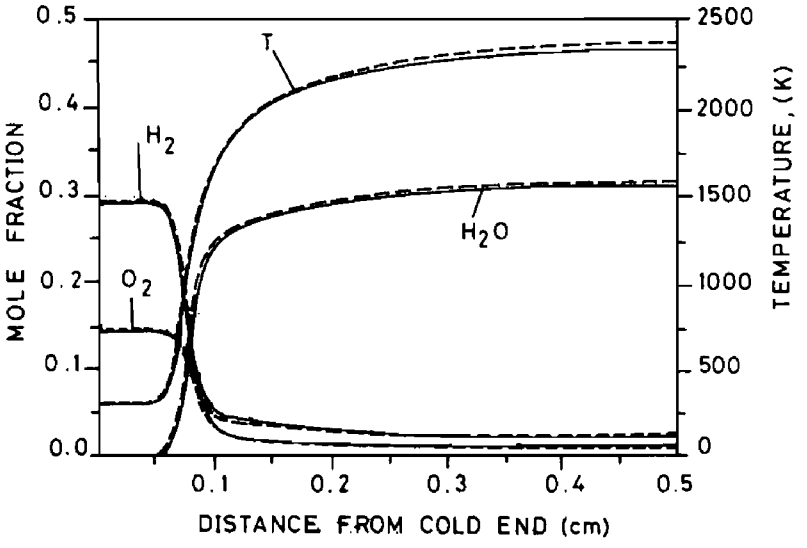

FIGURE 7 Profiles of T, H_2, O_2 and H_2O, present calculations (- - -) and those of Smooke *et al.* (1982b) (——) for a one atmosphere adiabatic H_2-Air flame.

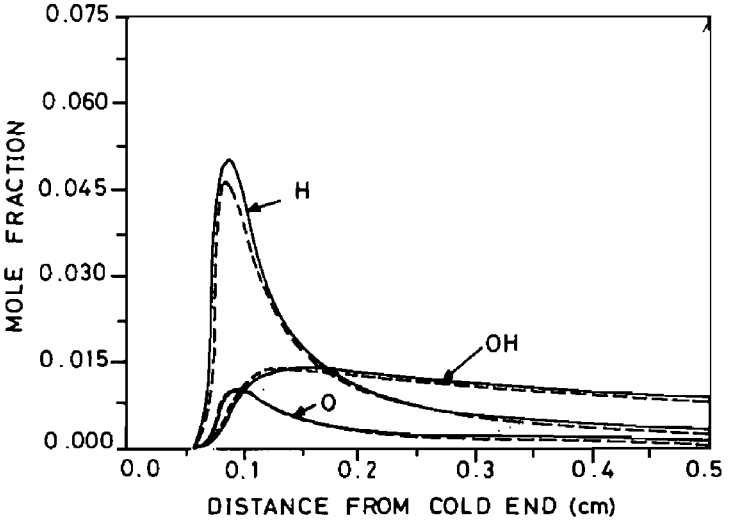

FIGURE 8 Profiles of O, H and OH, present calculations (- - -) and those of Smooke *et al.* (1982b) (——) for a one atmosphere adiabatic H_2-Air flame.

that the results of their computation using same kinetics lead to 1.81 m/s as the flame speed while it has been summarized by Warnatz in GAMM Workshop (1982) as 2.06 m/s. Some of the results of present study for H_2-Air flame in the light of Table 4 of summary paper by Warnatz (1982) are:

(1) V_u(m/s) = 2.03
(2) 10^3W(H, Max.) = 2.04
(3) 10^3W(O, Max.) = 6.64
(4) 10^4W(HO_2, Max.) = 7.2

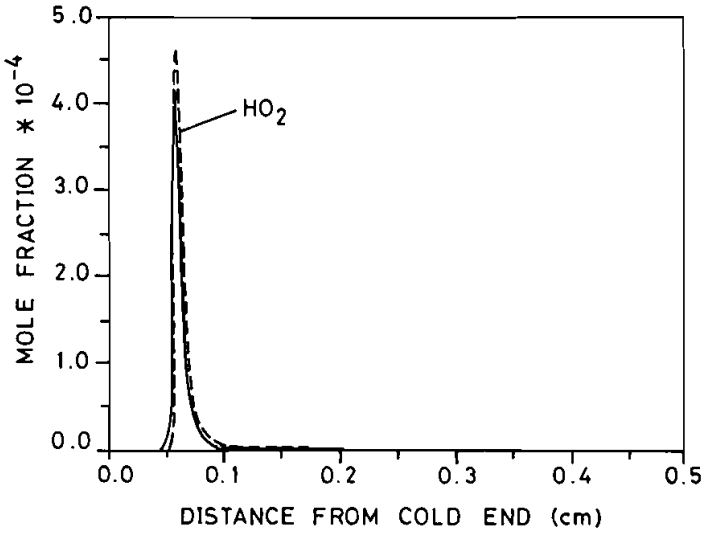

FIGURE 9 Profiles of HO_2, present calculations (- - -) and those of Smooke *et al.* (1982b) (——) for a one atmosphere adiabatic H_2–Air flame.

(5) $h_{max.}$(J/g) = 267
(6) $h_{min.}$(J/g) = −167
(7) Cells between 350 K and $0.9T_b$ = 18
(8) $n(HO_2)$ = 6 [With $X(HO_2)$ > 10% of maximum value.]
(9) Total no. of cells in computational domain = 50

4.2 *H_2–NO Flame*

Detailed computation of the flame structure of H_2–NO flame at various initial composition, initial temperature and pressures has been made. These show that the predicted results compared favourably with the experimental results given by Magnus *et al.*, (1974). For conditions: P = 1 Atmosphere, ϕ = 1, T_u = 1023 K, the predicted flame speed is 2.5 m/s about 10% higher than the experimental value measured by Magnus *et al.* (1974). Other results are reported separately (see Goyal *et al.*, 1988).

5 CONCLUSIONS

Present study examines many aspects related to the methods used for solution of premixed flame propagation problem. From the studies on two different systems H_2–Air and H_2–NO, the following are the main conclusions:

(1) The combination of an explicit diffusion operator and an implicit chemistry operator has been shown to provide a robust and convergent algorithm for adiabatic freely propagating one-dimensional premixed flames. This combination has possible implications for extensions to multi-dimensional problems.

(2) The robustness of the algorithm has been demonstrated by trying it on fairly simple and easily constructable initial profiles by taking H_2–Air and H_2–NO systems. All the cases tried converge to the steady state in 350 to 500 time steps.

(3) Pending a detailed stability study of the scheme, a simple method for computing cell size and time step has been given for adequate flame thickness resolution and convergence.

(4) It has been found that both the split and the unsplit schemes with explicit–implicit treatment for diffusion and chemistry are almost equally efficient in view of the near equality of the operation count involved in both the schemes. For complex chemistry however, the split scheme has a slight edge over the unsplit scheme.

(5) Trace diffusion approximation (Model D) with the correction in diffusion velocity due to Oran and Boris (1981) is a good substitute of multicomponent diffusion model which takes 15% more CPU time compared to the trace diffusion approximation.

ACKNOWLEDGMENTS

The authors are grateful to the referees for their comments and suggestions which have considerably enhanced the quality of the paper. H. S. Mukunda is currently NRC Research Associate, NASA Langley Research Center, Hampton, VA23665. Correspondence should be addressed to P. J. Paul.

REFERENCES

Andersson, L. L. and Olsson, J. O. (1986). A fast time-dependent code for evaluation of experimental premixed laminar flames. *Combustion Science and Technology* **46**, 95.

Bhashyam, A. T. (1984). Computational studies on problems of flame propagation. Ph.D. Thesis submitted in Indian Institute of Science, Bangalore, India.

Bhashyam, A. T., Deshpande, S. M., Mukunda, H. S. and Goyal, G. (1986). A novel operator-splitting technique for one-dimensional laminar premixed flames. *Combustion Science and Technology* **46**, 223.

Brokaw, R. S. (1961). Alignment charts for transport properties viscosity and diffusion coefficients for nonpolar gases and gas mixtures at low density. Report No. NASA TR R-81.

Coffee, T. P. and Heimerl, J. M. (1981). Transport Algorithm for premixed, laminar steady-state flames. Combustion and flame. **43**, 273–289.

Curtiss, C. F. and Hirschfelder, J. O. (1949). Transport properties of multicomponent gas mixtures. *J. Chem. Phys.* **17**, 550.

Dasch, C. J. and Blint, R. J. (1983). An improved Spalding–Stephenson procedure for one dimensional flame calculations. *Combustion Science and Technology* **34**, 91.

Dongarra, J. J. (1985). Performance of various computers using standard linear equations software in a Fortran environment. *Computer Architecture News*. Vol. **13**, No. 1, March 1985, p. 3.

Dwyer, H. A. and Sanders, B. R. (1978). Numerical Modeling of Unsteady Flame Propagation, Sandia Laboratories Report SAND77-8275.

Flower, W. L., Hanson, R. K. and Kruger, C. H. (1974). Kinetics of the reaction of nitric oxide with hydrogen. Fifteenth Symposium (International) on Combustion, The Combustion Institute, pp. 823–832.

Gordon, S. and McBride, B. J. (1971). Computer program for calculation of complex chemical equilibrium compositions, rocket performance, etc., Report No. NASA SP-273.

Goyal, G., Paul, P. J., Mukunda, H. S. and Deshpande, S. M. (1988). Computational studies on one-dimensional laminar, premixed Hydrogen–Nitric Oxide flames (communicated to Combustion and Flame, 1988).

Grcar, J. F., Kee, R. J., Smooke, M. D. and Miller, J. A. (1986). A Hybrid Newton/Time-Integration procedure for the solution of steady, laminar, one-dimensional flames. Sandia Laboratories Report SAND 85-8909.

Kee, R. J. and Miller, J. A. (1977). A split operator, finite difference solution for axisymmetric laminar jet diffusion flames, AIAA paper 77-639, AIAA 3rd computational fluid dynamics conf., June 1977.

Lund, C. M. (1978). HCT-a general computer program for calculating phenomena involving one-dimensional hydrodynamics, transport and detailed chemical kinetics. Univ. of California, Lawrence Livermore Report UCRL-52204.

Magnus, A. J., Chintapalli, P. S. and Vanpee, M. (1974). Effect of composition and temperature on the burning velocity of the Nitric Oxide–Hydrogen flame. *Combustion and flame* **22**, 71–75.

Olsson, J. O. and Andersson, L. L. (1985). Time-dependent solution of pre-mixed laminar flames with a known temperature profile. *Journal of Computational Physics* **59**, 369.

Oran, E. S. and Boris, J. P. (1981). Detailed modeling of combustion systems. Prog. in *Energy and Combustion Science*. **7**, 1.

Otey, G. R. (1978). Numerical methods for solving reaction–diffusion problems. Sandia Livermore Laboratories, Report No. SAND 78-8025.

Reitz, R. D. (1980). Computations of Laminar Flame Propagation Using an Explicit Numerical Method, 18th Symposium (International) on Combustion, The Combustion Institute, pp. 433–442.

Smooke, M. D. (1982). Solution of burner-stablized pre-mixed laminar flames by boundary value methods. *Journal of Computational Physics* **48**, 72.

Smooke, M. D., Miller, J. A. and Kee, R. J. (1982a). On the use of adaptive grids in numerically calculating adiabatic flame speeds. In Numerical Methods in Laminar Flame Propagation, N. Peters and J. Warnatz (Eds.), (GAMM Workshop Vol. 6), Friedr. Viewag and Sohn, Wiesbaden.

Smooke, M. D., Miller, J. A. and Kee, R. J. (1982b). Numerical solution of burner-stabilized premixed laminar flames by an efficient boundary value method. In Numerical Methods in Laminar Flame Propagation, N. Peters and J. Warnatz (Eds.), (GAMM Workshop, Vol. 6), Friedr. Vieweg and Sohn, Wiesbaden.

Smooke, M. D., Miller, J. A. and Kee, R. J. (1983). Determination of adiabatic flame speeds by boundary value methods. *Combustion Science and Technology* **34**, 79.

Warnatz, J. (1978a). Calculation of the structure of laminar flat flames, I. Flame velocity of freely propagating ozone decomposition flames. *Ber. Bunsenges. Phys. Chem.* **82**, 193.

Warnatz, J. (1978b). Calculation of the structure of laminar flat flames, II. Flame velocity and structures of freely propagating hydrogen-oxygen and hydrogen-air flames. *Ber. Bunsenges. Phys. Chem.* **82**, 643.

Warnatz, J. (1982). Discussion of Test Problem B. In Numerical Methods in Laminar Flame Propagation, N. Peters and J. Warnatz (Eds.), (GAMM Workshop, Vol. 6), Friedr. Vieweg and Sohn, Wiesbaden.

Yanenko, N. N. (1971). The method of fractional steps. Springer–Verlag, New York.